Local spectroscopy of Landau levels in mesoscopic Hall bars

O. Couturaud,[1] S. Bonifacie,[1] B. Jouault,[1] D. Mailly,[2] A. Raymond,[1] and C. Chaubet[1]
[1]*Groupe d'Etude des Semiconducteurs, UMR CNRS–Université Montpellier 2, 34090 Montpellier, France*
[2]*LPN–CNRS, site d'Alcatel, Route de Nozay, 95000 Marcoussis, France*
(Received 21 April 2009; published 21 July 2009)

We performed a local spectroscopy of the Landau levels density of states using gated mesoscopic Hall bars placed at very low temperature in the integer quantum Hall regime. The transverse and longitudinal conductances were measured while scanning both the two-dimensional electron density and the applied magnetic field. We observe a succession of sharp peaks due to backscattering across the samples caused by tunneling effects. Using temperature as a parameter in the range of 0.1–1 K, we characterize those tunnel processes: a resonant double-barrier tunneling and a single-barrier tunneling which corresponds to the variable range hopping regime. We show that for vanishing temperature and noninteger filling factor ν the conductance $\sigma(T=0,\nu)$ does not vanish unlike the case of wide samples: instead, it converges to a limit function $\sigma_S(\nu)$ that is a noisy image of the Landau levels density of states.

DOI: 10.1103/PhysRevB.80.033304 PACS number(s): 73.43.−f, 73.23.−b

In standard Hall bars whose widths are several tenths of microns, the quantum Hall effect (QHE) plateaus are sufficiently quantized due to the absence of backscattering,[1] to allow the conservation of the Ohm's etalon.[2] However, in mesoscopic Hall bars, fluctuations appear in both Hall resistance (R_H) and longitudinal resistance (R_L) in a large region between Hall plateaus due to backscattering between both edges of the mesoscopic sample.[3,4]

The first astonishing characteristic of these fluctuations, revealed by Cobden *et al.*[3] and Machida *et al.*,[4] is that one observes parallel lines along two directions when plotting $R_L(B,N_s)$ in a three-dimensional diagram as in Fig. 1(a) [where B is the magnetic field and N_s is the two-dimensional (2D) electron density]. This behavior has been attributed to charging effects[3] or modifications of the network of compressible and incompressible regions.[4] Recently, Ilani *et al.*[5] found similar lines but all of them parallel to one direction when measuring the compressibility of the 2D electron gas (2DEG). This effect is more pronounced at the plateaus center, where the filling factor ν is an integer and the density of states (DOS) vanishes, i.e., when adding an electron costs a finite energy. Thus the peaks observed by Ilani *et al.* represent the charging of the localized compressible puddles of electrons, as in conventional Coulomb blockade experiments. Very recently, Sohrmann *et al.*[6] showed via simulations that in the case of Ilani *et al.* the Coulomb interaction modifies the width of the compressible states and, consequently, the contrast of the lines observed in their experiments. In our experiments, as in the experiments of Cobden *et al.* and Machida *et al.*, we are concerned with the transition regions between Hall plateaus, where the filling factor ν is half-integer. The second astonishing characteristic of these conductance fluctuations, revealed by Peled *et al.*,[7] is the existence of correlations between the Hall resistance $R_H(B)$ and the longitudinal resistance $R_L(B)$. Zhou *et al.*,[8] by using a single-electron model based on a generalization of the Landauer-Buttiker formula,[1] demonstrated that these correlations reflect the symmetry of the diffusion matrix, a direct consequence of the chirality of the conduction processes that govern these fluctuations.

So, two aspects of the phenomenon are entangled and finally not contradictory: following Zhou *et al.*,[9] the correlations observed by Peled *et al.* can be understood in the general theory of the one-electron S matrix; following Sohrmann *et al.*, the visibility of the quantized lines in the (B,N_s) plane reflects the nontrivial screening ability of the 2DEG at mesoscopic scale,[10] which depends on the ratio between the strength of the Coulomb interaction and the disorder potential.[6]

Here we interpret the conductance fluctuations as a one-electron tunneling effect between incompressible puddles at integer ν. The characteristics of the tunnel process depend on the topology of the electron puddles.[4,5] However, to support this interpretation, it was necessary to identify definitely the conductance fluctuations with the transport mechanisms proposed by Zhou *et al.* In order to quantify precisely the hopping regime as well as the double-barrier tunneling, we have varied the temperature in the range for k_BT to scale the fundamental energies.

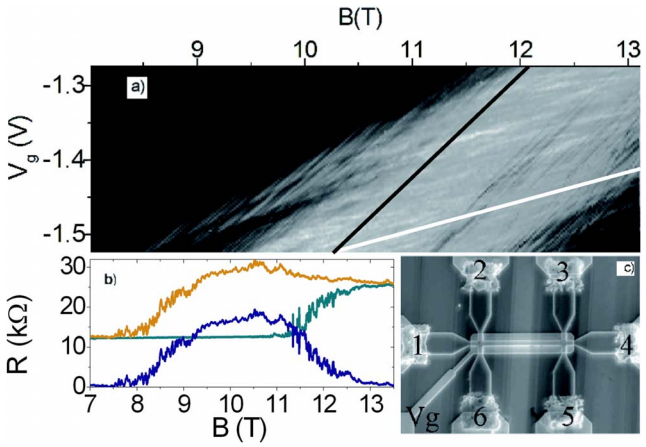

FIG. 1. (Color online) (a) In the B-n_s plane, the fine structure of the plateau-to-plateau transition appears as two series of entangled lines whose slope is quantized. Lines are guide for the eyes: $\nu=2$ in black, $\nu=1$ in white. (b) In blue (dark gray) $R_L=R_{14,23}$, in green (gray) $R_H=R_{14,62}$, and in orange (light gray) R_L+R_H, showing both correlated and noncorrelated regime. (c) Photo of the 13 μm-long TH1.5.

In this Brief Report we report experimental results obtained on mesoscopic Hall bars in the QHE regime in the temperature range 0.1–1 K. We tuned the top-gate voltage (V_g) and we characterized the tunneling processes that govern the conductance fluctuations of two categories of peaks, which we distinguish using the symmetry of the S matrix: those for which $R_L(B)$ and $R_H(B)$ are correlated, and those for which no correlation is observed. We identify unambiguously both kinds of tunnel mechanisms by their temperature dependence and we confirm the theory of Zhou *et al.*[8,9]

An unexpected consequence arises from our temperature dependence analysis: the longitudinal conductivity as a function of V_g follows the shape of the Landau levels (LL's) DOS, though it deviates from the true DOS by sharp peaks whose origin is understood. Therefore, we have realized a local LL spectroscopy of a small part of the GaAlAs/GaAs heterojunction.

Measurements were performed using standard lock-in amplifier techniques at 7 Hz, by applying a voltage drop across the sample smaller than 10 μV, so that we always verified the condition $eV < k_BT$. We performed experiments on several samples processed on a same GaAs/InGaAs/GaAlAs heterostructure. At 4.2 K, the two-dimensional electron gas in the quantum well has a carrier density $N_s = 9 \times 10^{11}$ cm^{-2} and a mobility of 3 m^2/V s. The wafer is patterned into Hall bars of different dimensions having a gate on top to modulate the electron concentration of the 2DEG [see Fig. 1(c)]. Due to the very thin spacer between the δ-doping layer and the 2DEG (4 nm), the 2DEG is strongly perturbed by the ionized impurities and the LL's develop a broad low-energy tail.[11] A clear experimental signature of the asymmetry of LL's is the shift of the Hall plateaus toward lower B: the line of the classical resistance $R_{\text{class}} = B/N_s e$ does not cross the middle of the Hall plateaus[12] and, as shown by Fig. 1(b), the minima of the Shubnikov–de Haas (SdH) curve do not correspond exactly with the plateaus.[13] Another cause of asymmetry of the density of states for our narrowest samples is the formation of a quantum wire due to the lateral confinement. This results in a high-energy tail caused by the important weight of the states close to the edges in these samples.[14] Our results are obtained on narrow Hall bars of width 1.5 μm (TH1.5) and 2 μm (TH2). Moreover, a depletion zone on both sides of the Hall bar due to the etching process reduces also the effective width W^* of the 2DEG:[13] for instance, for TH1.5, $W^* = 420$ nm at $V_g = 0$ V, and $W^* = 150$ nm at $V_g = -1.5$ V.

In Fig. 1, we distinguish two categories of fluctuations using the Zhou classification: (1) First, on the low-B (or high-ν) side of the SdH peaks, fluctuations occur in the R_L resistance while R_H remains quantized. Those tunneling mechanisms are chiral and are described in the theory of Zhou by the resonant double-barrier tunneling between edge states, using antidots in the middle of the bar as intermediate states.[15] In the (B, N_S) plane, those fluctuations draw lines parallel to the slope $\nu = 1$ [see Fig. 1(a)], which signifies that the localized intermediate antidot is an incompressible puddle at $\nu = 1$ [see Fig. 2(a)]: when (B, N_S) vary, the conductance value at the resonance peak remains the same as long as the shape of the $\nu = 1$ puddle remains the same.[16] Thus, the resonance peak moves like $\nu = 1$. (2) Second, correlated fluctuations between R_L and R_H appear on the high-B side of the SdH peaks verifying $R_L + R_H = h/e^2$, which signifies that the S matrix is symmetric. According to Zhou *et al.*, these fluctuations are due to hopping between localized puddles of same ν passing through hills of potential at filling factor $\nu = 1$ [see Fig. 2(b)]. The hopping conductivity, resulting from the recovery of the tails of the wave functions,[17] would then be the consequence of a multiple tunneling process through single barriers formed by the hills of the disorder potential. In the plane (B, N_S) in Fig. 1(a), those lines move parallel to $\nu = 2$ (Ref. 13) supporting the interpretation that the shape of the incompressible puddles at $\nu = 2$ is the relevant parameter for the hopping conductance.

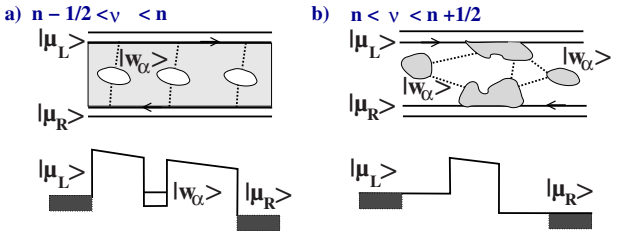

FIG. 2. (Color online) Mechanisms proposed by Zhou having the appropriate symmetry (black: contacts; gray: incompressible fluid at $\nu = 2$; white: incompressible fluid at $\nu = 1$). (a) The Jain Kivelson process is a double-barrier tunneling. (b) The hopping regime corresponds to a multiple single-barrier tunneling.

In Fig. 3, we report the normalized conductance $\sigma_{xx}/(e^2/h)$ [where σ_{xx} is approximated to $(W^*/L) \times (R_L/R_H^2)$ because $R_L \ll R_H$] for different temperatures in the range 0.1–1 K. We tuned the magnetic field to scan the transition $(\nu = 2 \rightarrow 1)$. It is obvious that the opposite side of the transition on the B axis has a different behavior with increasing temperature. In the inset, we have enlarged a part of the low-B side: we observe that the amplitude of the major peak decreases when the temperature increases while the peak is broadening. Contrarily, on the high-B side of the transition, the mean value of the conductance increases when the temperature increases, showing that a different mechanism controls the conductance. In the following we analyze the temperature dependence of both categories of peaks.

On the low-B part of the SdH transition, the peak height decreases with increasing temperature as shown in the inset

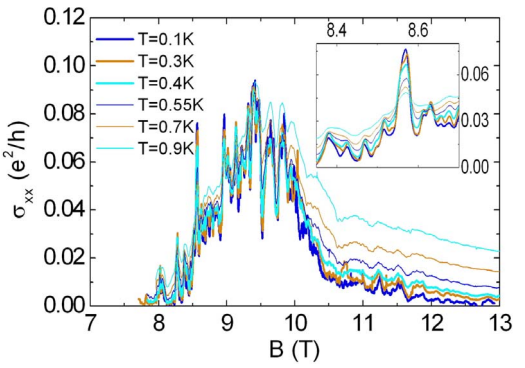

FIG. 3. (Color online) Normalized conductivity for the transition $(\nu = 2 \rightarrow 1)$ and different temperatures in the range 0.1–1 K for sample TH2. In the inset, a zoom on the Jain Kivelson peaks.

of Fig. 3 (see also Fig. 5 in our previous work[13]). This is the signature of a resonant double-barrier tunneling [see Fig. 2(b)] between edge states. The barrier height is a fraction of the energy gap between the first and the second LL ($\hbar\omega_c$ =16 meV at 10 T) because the energy of the lowest free electronic state above the incompressible fluid $\nu=2$ lies in the next Landau level.

In our experimental conditions, the longitudinal conductivity σ_{xx} corresponds exactly to the conductance between edge states. Considering a single energy level $|w_\alpha\rangle$, we call Γ_L^α and Γ_R^α the transparencies of the tunnel barriers that isolate the state $|w_\alpha\rangle$. We define $\Gamma^\alpha=(\Gamma_L^\alpha+\Gamma_R^\alpha)/2$ and $\mathcal{A}_\alpha(E)$ as the spectral function, whose width is Γ^α, of the intermediate localized state at the energy E_α (see for example Ref. 18). Following Bruus and Flensberg,[19] the total double-barrier conductance through the dots including Coulomb interactions is

$$\frac{\sigma_{xx}}{\sigma_0}=\int_E \frac{dE}{2\pi}\left(-\frac{\partial f}{\partial E}\right)\sum_\alpha \frac{\Gamma_L^\alpha\Gamma_R^\alpha}{\Gamma_L^\alpha+\Gamma_R^\alpha}\mathcal{A}_\alpha(E). \quad (1)$$

For the lowest temperatures ($k_BT\ll\Gamma$), a straightforward calculation leads to

$$\sigma_{xx}/\sigma_0=\frac{1}{2\pi}\sum_\alpha \Gamma_\parallel^\alpha\mathcal{A}_\alpha(\mu), \quad (2)$$

where μ is the Fermi energy, $\sigma_0=2e^2/h$, and $\Gamma_\parallel^\alpha=(\Gamma_L^\alpha\Gamma_R^\alpha)/(\Gamma_L^\alpha+\Gamma_R^\alpha)$. Thus it is obvious that for sufficiently low temperature, the longitudinal conductance reveals the complete local density of states. However, the true shape is distorted by the maxima of the prefactor $\Gamma_\parallel^\alpha$ when the intermediate state $|w_\alpha\rangle$ is located right in the middle of the Hall bar.[15]

For higher temperature ($k_BT\gg\Gamma$), Eq. (1) leads to the formula $\sigma_{xx}/\sigma_0=(1/2\pi k_BT)\Sigma_\alpha\Gamma_\parallel^\alpha\cosh^{-2}(\frac{E_\alpha-\mu}{2k_BT})$. We have fitted a great number of peaks with the usual law[20] $\sigma_{xx}/\sigma_0=G_T\cosh^{-2}(\frac{V_g-V_0}{W(T)})$ and found $W(T)$ and G_T for each temperature. In Fig. 5 of Ref. 13, we have for example characterized completely one peak; we have shown that above 300 mK, the width $W(T)$ increases like k_BT as expected, whereas below 300 mK, the width of the transition is almost constant. Similarly, the maximum G_T decreases like $1/k_BT$, as expected, but saturates below 300 mK. The temperature dependence of the conductance allows to scale the energy width of $|w_\alpha\rangle$ (Ref. 21): we obtain $\Gamma^\alpha\approx 30$ μeV and $\Gamma_\parallel^\alpha\approx 3$ μeV.

On the high-B part of the SdH peaks, the mechanism proposed by Zhou *et al.* is a hopping process from localized puddles $\nu=2$ to localized puddles at $\nu=2$ through the surrounding quantum Hall fluid at $\nu=1$ [see Fig. 2(a)]. Experimental results show that the temperature dependence of the conductivity is, in fact, perfectly represented by the sum of the variable-range hopping conductivity[17] and a constant $\sigma_S(\nu)$:

$$\sigma_{xx}(\nu,T)=\sigma_S(\nu)+\sigma_H(T)\exp(-\sqrt{T_0/T}), \quad (3)$$

where the prefactor $\sigma_H\propto 1/T$. For several couples (B,V_g), we have plotted the conductivity $\sigma_{xx}(\nu,T)$ as a function of the temperature in order to obtain the quantity $\sigma_S(\nu)$. This allowed us to report in Fig. 4(a) the quantity $T[\sigma_{xx}(\nu,T)-\sigma_S(\nu)]$ as a function of $\sqrt{T_0/T}$ on a semi-log scale. We obtain a linear dependence with a slope that varies slightly with the filling factor. This dependence is a clear signature of the variable-range hopping process in QHE conditions and we obtain the localization length ξ by using the formula[22] $k_BT_0=(6\times e^2)/(4\pi\varepsilon\xi)$.

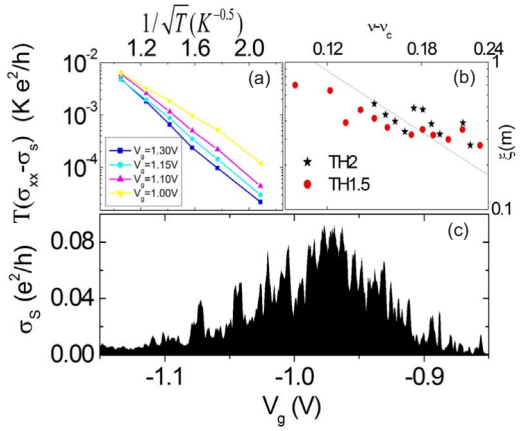

FIG. 4. (Color online) (a) Hopping conductivity as a function of the temperature for TH2. (b) Localization length as a function of $(\nu-\nu_c)$. The straight line corresponds to the expected universal law $\xi(\nu)=(\nu-\nu_c)^{-2.3}$. (c) Sample TH2 at $B=13.5$ T. The conductivity at $T=0.1$ K is an image of the asymmetrical DOS.

We have reported the values of ξ as a function of $\nu-3/2$ in Fig. 4(b). Contrary to the case of wide samples for which a clear linear dependence with a slope 2.3 is measured,[23] we observe for narrow samples that data are scattered around the universal law $\xi(\nu)\propto(\nu-\nu_c)^{-2.3}$ and that the slope is smaller than the expected value. Now, the localization length is comparable to the width of the sample (for TH2, $W^*\approx 600$ nm at $V_g=-1.3$ V), and we attribute both the dispersion of our data in Fig. 4(b) and the reduced value of the critical exponent to the geometrical constraint imposed on the extension of electronic wave functions.

Finally, let us return to the skeleton function $\sigma_s(\nu)$, which is the limit of the SdH curve at vanishing temperature, represented in Fig. 4(c) by the black area obtained at $T=0.1$ K. In wide samples, the conductivity vanishes at vanishing temperature, except at the center of the SdH peaks.[24] In narrow samples, the recovery $\langle\mu_L|\mu_R\rangle$ of the electronic wave function from reservoir $|\mu_R\rangle$ to reservoir $|\mu_L\rangle$ (see Fig. 2) is enhanced by the distribution of localized states $|w_\alpha\rangle_\alpha$ of energy E_α, which participate in the total transmittance if the Fermi energy $\mu=E_\alpha$. The total transmission $T=|\Sigma_\alpha\langle\mu_L|w_\alpha\rangle\langle w_\alpha|\mu_R\rangle|^2$ can be developed as

$$T=\sum_\alpha |C_{L,\alpha}|^2|C_{R,\alpha}|^2+\sum_{\alpha,\alpha'\neq\alpha} C_{L,\alpha}C_{L,\alpha'}^*C_{R,\alpha}^*C_{R,\alpha'}, \quad (4)$$

where $C_{L(R),\alpha}=\langle\mu_{L(R)}|w_\alpha\rangle$. The first term decreases as $\exp(-\xi/W)$ and vanishes in wide samples. However, in our narrow samples, it is proportional to the number of states at the energy E_α. Thus, as for the high-ν side of the transition, the longitudinal conductivity is proportional to the local DOS.

Therefore, and this appears clearly in Fig. 4(c), the conductivity at vanishing temperature, the black asymmetrical area, gives a noisy image of the density of states.[25] Indeed, the density of states characterizes the disorder and thus the sample itself; therefore, only the smooth envelope of the conductivity at $T=0$ can be independent of the measurement method and can represent the mean DOS of the sample. Contrarily, all the peaks superimposed on this smooth structure reveal the local impurity concentration and depend, of course, on the pair of contacts used in the transport measurements. The peaks on the right side are due to the enhancement of the prefactor in Eq. (1). Moreover, the second term in Eq. (5), resulting in interferences between different paths, could be at the origin of the oscillations which appear on the left side of the black area in Fig. 5(c) in Ref. 26. For this heterojunction, it appears clearly that the DOS is asymmetric. This confirms the results of the calculations made by Bonifacie *et al.* (see Ref. 11) on this kind of heterostructure. In high mobility samples, the DOS might be more narrow in energy and less asymmetric.

In conclusion, by studying the temperature dependence of the conductance fluctuations in mesoscopic Hall bars, we have identified a double-barrier tunneling and a multiple single-barrier tunneling. The mesoscopic Hall bar, when measuring the longitudinal conductivity across the SdH transition, plays the role of a local probe and gives an image of the density of states.

This work was financed by the French National Agency for Research (ANR). We thank Ken Ichiro Imura from Tohoku University for enlightening discussions.

[1] M. Buttiker, Phys. Rev. B **38**, 9375 (1988).
[2] R. E. Prange and S. M. Girvin, *The Quantum Hall Effect* (Springer-Verlag, New York, 1990).
[3] D. H. Cobden, C. H. W. Barnes, and C. J. B. Ford, Phys. Rev. Lett. **82**, 4695 (1999).
[4] T. Machida, S. Ishizuka, S. Komiyama, K. Muraki, and Y. Hirayama, Phys. Rev. B **63**, 045318 (2001).
[5] S. Ilani, J. Martin, E. Tetelbaum, J. H. Smet, D. Mahalu, V. Umanski, and A. Yacobi, Nature (London) **427**, 328 (2004).
[6] C. Sohrmann and R. A. Römer, Phys. Status Solidi C **3**, 313 (2006); New J. Phys. **9**, 97 (2007).
[7] E. Peled, D. Shahar, Y. Chen, E. Diez, D. L. Sivco, and A. Y. Cho, Phys. Rev. Lett. **91**, 236802 (2003); E. Peled, D. Shahar, Y. Chen, D. L. Sivco, and A. Y. Cho, *ibid.* **90**, 246802 (2003).
[8] C. Zhou and M. Berciu, Phys. Rev. B **72**, 085306 (2005).
[9] C. Zhou and M. Berciu, Nat. Phys. **4**, 24 (2008).
[10] A. L. Efros, Solid State Commun. **70**, 253 (1989); **67**, 1019 (1988).
[11] S. Bonifacie, C. Chaubet, B. Jouault, and A. Raymond, Phys. Rev. B **74**, 245303 (2006).
[12] R. J. Haug, R. R. Gerhardts, K. V. Klitzing, and K. Ploog, Phys. Rev. Lett. **59**, 1349 (1987).
[13] B. Jouault, O. Couturaud, S. Bonifacie, D. Mailly, and C. Chaubet, Phys. Rev. B **76**, 161302(R) (2007).
[14] A. Struck, B. Kramer, T. Ohtsuki, and S. Kettemann, Phys. Rev. B **72**, 035339 (2005).
[15] J. K. Jain and S. A. Kivelson, Phys. Rev. Lett. **60**, 1542 (1988).
[16] See Fig. 3 in Ref. 3.
[17] Y. Ono, J. Phys. Soc. Jpn. **51**, 237 (1982).
[18] S. Datta, *Electronic Transport in Mesoscopic System* (Cambridge University Press, Cambridge, U.K., 1997).
[19] H. Bruus and K. Flensberg, *Many-Body Quantum Theory in Condensed Matter Physics* (Oxford University Press, New York, 2004), p. 165, Eq. (10.56).
[20] C. W. J. Beenakker, Phys. Rev. B **44**, 1646 (1991); I. Karakurt, V. J. Goldman, J. Liu, and A. Zaslavsky, Phys. Rev. Lett. **87**, 146801 (2001).
[21] The determination of Γ^{α} is independent of the capacitance of the gate; see I. J. Maasilta and V. J. Goldman, Phys. Rev. B **57**, R4273 (1998).
[22] M. Furlan, Phys. Rev. B **57**, 14818 (1998).
[23] F. Hohls, U. Zeitler, and R. J. Haug, Phys. Rev. Lett. **88**, 036802 (2002).
[24] The width $\Delta\nu$ of the SdH peaks scales like $\Delta\nu \propto T^{0.4}$ as shown by D. G. Polyakov and B. I. Shklovskii, Phys. Rev. Lett. **70**, 3796 (1993).
[25] P. T. Coleridge, P. Zawadzki, and A. S. Sachrajda, Phys. Rev. B **49**, 10798 (1994).
[26] Such oscillations appear identically while scanning B and an estimate of the area enclosed by wave functions that interfere is approximately $\Phi_0/\Delta B \approx 1\ \mu\text{m}^2$.